



# NUMERICAL AND EXPERIMENTAL STUDY ON THERMAL FLUID FLOW OVER TWIN DIAMOND-SHAPED CYLINDERS IN FREE STREAM

Shinzaburo Umeda<sup>1,C</sup>, Shuichi Torii<sup>2</sup>

<sup>1</sup> Department of Architecture and Civil Engineering, Fukuyama University,  
Fukuyama, 729-0292, Japan

<sup>2</sup> Department of Mechanical System Engineering, Kumamoto University,  
Kumamoto, 860-8555, Japan

<sup>C</sup> Corresponding author: Tel.: +81849362111; Fax: +81849362023;  
Email: s-umeda@fucc.fukuyama-u.ac.jp

## KEYWORDS:

**Main subject(s):** *experimental fluid mechanics, flow visualization*

**Fluid:** *air and water*

**Visualization method(s):** *PIV*

**Other keywords:** *flip-flop flow, streamwise diverging diamond-shaped cylinder bundle, concavity*

**ABSTRACT :** *The aim of the present research is to develop the fundamental study on the control of the self-excited oscillations in diamond-shaped cylinder bundles. The PIV measurements are performed on the flow visualization in the horizontal cross section of the exit jet-stream flow field exiting from diamond-shaped cylinder bundles. Comparison is carried out using the measured results in the absence or presence of the concavities constructed on both sidewalls inside the diamond-shaped cylinder bundle. It is found from the study that (i) velocity vectors are mutually spread on left or right direction at the angle of 30°, that is the diverging angle of the jet-stream from the bundle becomes 60°, (ii) the mean absolute values of the jet-stream velocity-variation rate,  $|dV/dy|$ , at the cross-section of the channel is increased for each bundle, and (iii) a substantial enhancement of  $|dV/dy|$  takes place at Type D60c for the streamwise diverging diamond-shaped bundle.*

## 1 Introduction

In various industrial devices such as fluid machinery and combustion equipment, the efficiency of mechanical performance may be enhanced by promoting jet-stream diffusion. Both active and passive means are constructed for the control of such jet streams. The corresponding numerous research works were presented. For example, Zaman et al. [1] applied vortex generators for controlling an axis-symmetrical method of generations and Yokota [2] developed a device for various generations by means of self-sustaining oscillations. In the decade of 1990's, the authors also studied the cross-sectional view of a flow network with a single intersection and a flow system consisting of mutually intersecting flow passages inside a plate or an assembly of plates. They reported the fundamental study

on a flip-flop flow of a single jet stream. In particular, Umeda and Yang [3] and Umeda et al. [4] discovered self-excited multiple jet-stream groups from diamond-shaped cylinder bundles. It was disclosed that these flow fields consisted of multiple jet streams of equal flow rates in the exit flow streams which is symmetrical with the central longitudinal line as the axis. When a flip-flop flow is generated from a diamond-shaped cylinder bundle, the von Karman vortices generated in both left- and right- rear-flow regions behind the cylinders undergo fluctuations. Furthermore, Umeda et al. [5] studied flip-flop flow oscillation from a diamond-shaped cylinder bundle with wall concavity. They disclosed that the presence of wall concavity results in a remarkable change in the jet-stream from the diamond-shaped cylinder bundle in higher turbulence levels and dispersion of individual jet-streams with respect to those without concavities [5].

In industrial applications of the exit oscillation jet streams, the diamond-shaped cylinder bundles provide an exit jet stream flow field with multiple equal flow-rate jet-stream group having self-excited oscillations and can be applied to fluids engineering machinery for mixing, stirring, diffusion, heat transfer and cleaning operations. Note that the corresponding flow fields and various devices require the improvement of further functions as advanced devices as:

- (1) although flip-flop flow is observed in the exit jet streams from the flow passages, its direction indicated oscillations is within 30 degree whose wideness is somewhat narrow.
- (2) a diamond-shaped cylinder bundle which consists of multiple rows of diamond-shaped cylinders with 30-degree apex angle in staggered arrangement, amplifies the pressure drop in the channel.

In order to develop the application device, furthermore development and pressure characteristics in the channel may be requested.

The flip-flop flow induced from the diamond-shaped cylinder bundles is observed in multiple rows of diamond-shaped cylinders with about 60-degree apex angle in staggered arrangement [7]. The presence of the flip-flop flow behavior appears inside the flow passage at the fourth row in the bundle. In other words, there is no effect of diamond-shaped cylinders over the fifth row in the bundle on the presence of flip-flop flow [8].

In the present work, in addition to the specific characteristics of a continuous intersecting flow of the converging and diverging flow of the main stream, a visualization study and a pressure measurement are performed on a diamond-shaped cylinder bundle revised with concavities on both bundle walls. Here, the revised channel with a diamond-shaped cylinder bundle is consisted of the fourth row bundles having an apex angle of 30°, diamond-shaped cylinders with an increase in 10° interval apex in the downstream direction, and eighth row bundle of diamond-shaped cylinders with having an apex angle of 60°. In order to determine whether or not self-excited oscillations induced by the intersecting of the main stream have a remarked changes due to the presence of the concavities, results are compared with those in the absence of the concavities.

## 2 Experimental Methods

### 2.1 Experimental apparatus

In the present study, five different diamond-shaped cylinder bundles are employed. As an example, an upper view of a diamond-shaped cylinder bundle revised with concavities on both bundle walls is illustrated in Fig. 1. The corresponding channel constructed with multiple rows of diamond-shaped cylinders is consisted of circular concavities on both channel walls at the fourth row in the bundle and

similar circular concavity on an upper channel wall between twin diamond-shaped cylinders at the fifth row in the bundle. This channel type is referred to as 'Type D60cu'. Different diamond-shaped cylinder bundles revised with concavities are summarized in Fig. 2. Here, Left upper part in the column is 'Type name' and an apex angle of  $30^\circ$  is named as 'D30'. Note that the revised channel with a diamond-shaped cylinder bundle with the fourth row bundles having an apex angle of  $30^\circ$  and eighth row bundle of diamond-shaped cylinders with having an apex angle of  $60^\circ$  is indicated as 'D60'. In order to distinguish the channel, the channel without concavities on both bundle walls, with concavities and with circular concavity on an upper channel wall corresponds to a subscripted name as 'n', 'c', and 'cn', respectively. The diamond-shaped cylinder bundle consisted of multiple rows of diamond-shaped cylinders in the flow direction and seven columns in the lateral direction. The number of rows is different by 'Type' and its number is indicated in the upper right of the column. The shape for 'Type' is illustrated in the center part of the column and the absence and presence of concavity are shown as 'Without concavity' and 'Concavity', respectively.

As for five different diamond-shaped cylinder bundles, since the substantial narrow flow cross-section easily causes the flip-flop flow, the square duct shape in which the channel height  $d$ , short axis width of diamond-shaped cylinder and narrow flow cross-section width is the same as 5mm, is employed.

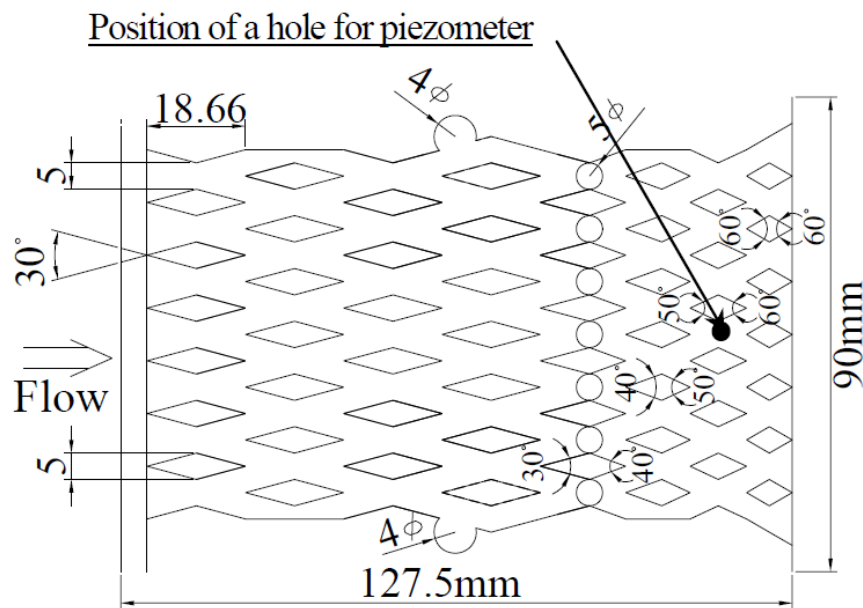


Fig. 1 Top view in a diamond-shaped cylinder bundle (Type D60cu)

## 2.2 Measurement of water jet

The experimental setup consisted of an upstream head tank with head of  $H_u$  to supply the test liquid, water, a flow calming section, a test section, a measuring section, a downstream collection tank, and a pump to re-circulate the flow. A digital camera was used for recording water jet streak-lines exiting from the cylinder bundle and path lines inside the flow passages. The tracer used in the visualization of path lines was high-porous polymer particles of approximately from 200 to 350  $\mu\text{m}$  in diameter.

In order to measure the pressure drop in the five different channel employed here, the head  $H_u$  of the upstream head tank was varied to change flow rates through the test section and  $P_d/\rho g$  at the seventh row of diamond-shaped cylinders was estimated. The corresponding location is shown in Fig. 1 as the

‘•’ which is the narrow channel cross-section at the seventh row of diamond-shaped cylinders. The inlet flow rate was varied in term of the Reynolds number  $Re$ , which was defined based on the averaged velocity  $U$  at the flow cross section of the upstream duct as the characteristics velocity and the passage thickness  $d$  as the characteristics length.

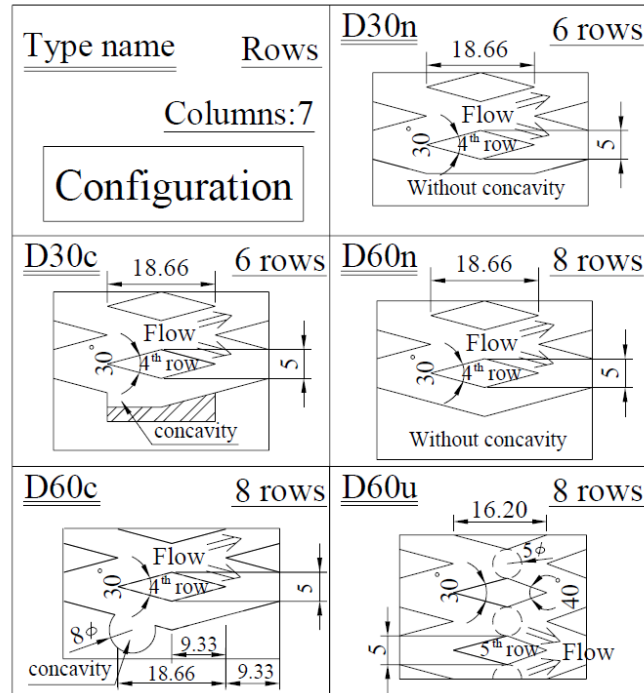


Fig. 2 Kinds of configurations around a right side wall at 4th or 5th row in diamond-shaped cylinder bundles

### 2.3 PIV measurement with the aid of air jet stream

In case of using air as the test fluid, a rectified-flow passage was needed upstream of the diamond-shaped cylinder bundle in order to generate flip-flop flow. Therefore, a flow-calming section was installed to supply air from a blower, as illustrated in Fig. 3. The coordinate system of the flow measurement is superimposed in Fig.3. The co-ordinate system was provided identifying the location in the measuring region, as shown in Fig. 3. The origin of the co-ordinate system is set at the center of the exit from the diamond-shaped cylinder bundle, measuring the flow direction by the x-axis, the lateral direction by the y-axis, and the vertical direction by the z-axis.

For visualizing air jet streams, PIV measurements (LaVision Co.) were performed in the measuring region, i.e., the horizontal area of  $x=10\sim 100\text{mm}$  and  $Z=0\text{mm}$ . Here, the horizontal direction corresponds to the width of the flip-flop flow, that is Type D30n and D30c is  $y = \pm 20$  and the others is  $y = \pm 30$ . In case of supplying air from a blower, a smoke generator was installed at the suction port to simultaneously supply a tracer for the PIV.

Results of the PIV measurements were recorded using a CCD camera with the sampling frequency of 15 Hz, the pulse interval of 25  $\mu\text{s}$ , and the pixel number of 1340 by 1040. Vector images 500 frames in which one vector is estimated by 32x32pixel, were obtained.

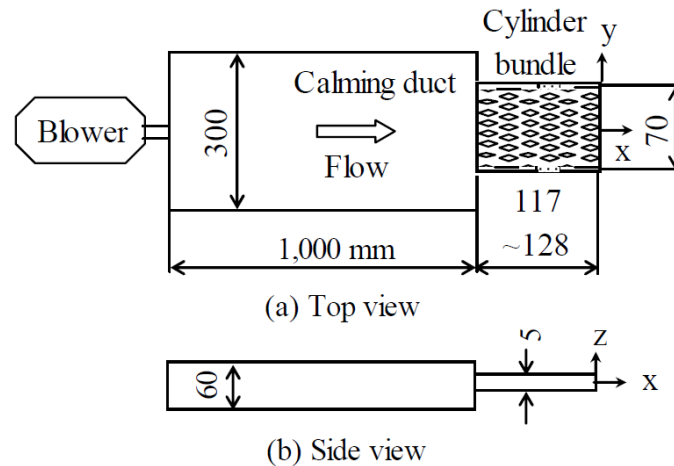


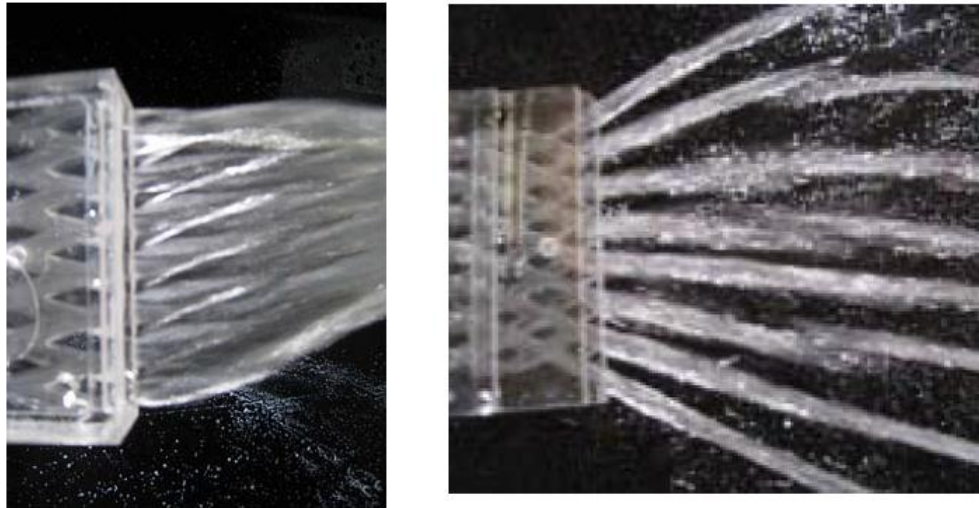
Fig. 3 Schematic diagram of the experimental setup

### 3 Experimental Results and Discussion

#### 3.1 Visualization and flow measurement of water jet streaklines

A digital camera was employed to record the streakline photograph of water jet streams exiting from diamond-shaped cylinder bundles with and without wall concavity. Representative results are presented in Figs. 4(a) and (b) for the with- and without- wall-concavity cases and the channel flows with-concavity are depicted in in Figs. 5(a) and (b) with the aid of the tracer flow visualization method. In each case, flip-flop flow was observed in the exit jet streams from the flow passages. Figure 4 observes that in the absence of wall concavity, the visualization results observed from the top direction causes oscillations of the streaklines (Fig. 4(a)), while wider oscillation of the streaklines is induced due to the presence of wall concavity (Fig. 4(b)). This twisting characteristics of the flow was slightly affected by the concavity location, i.e., Type D60c and Type D60cu. In other words, the consequences of installing a wall concavity on the exiting jet flow streaklines include (i) oscillations of flip-flop flow, (ii) enhancement of jet stream dispersion in both the left and right direction, and (iii) growth in the twisting and turbulence of the jet streams.

As to the different twisting behavior, the exiting jet stream characteristics are caused by the wake behind the diamond-shaped cylinder and the suction effect which is performed as longitudinally rotating. This tend becomes clearer in Fig. 5 (a) and (b). These photos reveal the path lines near the wall concavities. As for Type D60c, one can identify the formation of vortices inside the wall concavity which is shown in Fig. 5(a) as the dotted line. In other words, a rotating vortex appears (although less clearly) in the upstream side of the wall concavity and causes the suction effect [6] in the intersecting region and the vortex movement behind the diamond-shaped cylinder. Consequently, the suction effect is induced to act at the wall concavity, resulting in pulling its neighboring jet stream toward the wall concavity. It is anticipated that the pulling phenomenon would change by designing the shape of the downstream part of the wall concavity. Hence, by inducing the suction motion at the wall concavity, it is possible to change not only the flow of the exiting jet streams but also the flow in the exiting jet-stream field with enhanced dispersion and turbulence.



(a) Type D30n (Re=7,400)

(b) Type D60cu (Re=7,500)

Fig. 4 Visualization of jet streams at an instant time

The slight different flip-flop flow is observed in the case of Type D60cu, as seen in Fig. 5(b). The channel constructed with multiple rows of diamond-shaped cylinders is consisted of circular concavities on both channel walls at the fourth row in the bundle and similar circular concavity on an upper channel wall between twin diamond-shaped cylinders at the fifth row in the bundle, as mentioned previously. The corresponding area of circular concavity on an upper channel wall is shown in Fig. 5(b) as the white dotted circular line. One observes that a few white particles which depict the rotating motion appear. It is postulated, therefore that this movement and the suction motion at the wall concavity are interacted together, resulting in the slight enhancement of flip-flop flow.

Figure 6 illustrates the pressure loss coefficient,  $C_p$ , versus the Reynolds number,  $Re$ , for different five channels with diamond-shaped cylinder bundles. Here  $C_p$  is defined as:

$$C_p = (H_u - P_d / \rho g) / (U^2 / 2g) \quad (1)$$

It is observed that the pressure loss coefficient is lineally decreased with an increase in the Reynolds number. Notice that the  $C_p$  for Type D30c, at  $Re$  fixed, is lower than that for the other Types. This is because the pressure loss coefficient is affected by the shape and size of the concavities on channel walls. In contrast, higher pressure loss coefficient occurs for Type D60cu, because the number of concavities increases. Similar value shows for D60c in the low Reynolds number region, while  $C_p$  agrees with that for D30c in the high Reynolds number region. It is found that the pressure loss in the channel is affected by the shape and size of the concavities and the Reynolds number.



(a) Around a right side wall at 4<sup>th</sup> row for Type D60c (Re=7,600)



(b) Around a center at 5<sup>th</sup> row for Type D60cu (Re=7,500)

Fig. 5 Visualization of path lines from top view

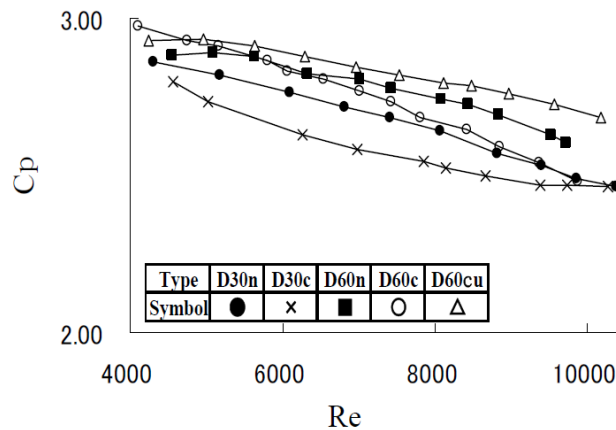


Fig. 6 Change of Cp versus Re

### 3.2 Visualization and flow measurement of air jet streaklines

The blower installed at the upstream side was operated at the inverter control frequency between 10 Hz and 30 Hz. Air jet-stream velocity exiting from diamond shaped-cylinder bundles with wall concavity varied substantially depending on location.

The jet-stream velocity fields in the vicinity of the channel exit were employed in the PIV measurements. Among the results obtained for the velocity, the instant velocity vectors at two different times are illustrated in Figs. 7.1 (a) and (b) in the case of Type D30n and Re=7900. The similar velocity vectors are depicted in Figs. 7.2 (a) and (b) in the case of Type D60cu and Re=7300. For reference, the gradient, i.e., 15o and 30o are indicated at y=0.

As mentioned previously, oscillations of flip-flop flow and jet stream dispersion in both the left and right direction are different for Type D30n and Type D60cu. In other words, enhancement of jet

stream dispersion is caused for Type D60cu than Type D30n and its dispersion angle is  $60^\circ$ , as seen in Fig. 7.2.

For the without and with -wall-concavity case, average equi-velocity distribution and average iso- $dV/dy$  distribution on the horizontal cross section were plotted in Figs. 8.1(a) and 8.2(a). Here, the average velocity is obtained based on the instant velocity image data in the PIV measurements. In regard to the mean flow velocity in the lateral direction  $V$ , equi- $dV/dy$  distribution is presented in Figs. 8.1(b) and 8.2(b). For both with- and without-wall concavity, the generation of flip-flop flow caused the flow to be nearly symmetrical with respect to the central longitudinal line of the exit jet-stream flow field. For the without wall-concavity case, i.e., for Type D30n, both the flow velocity difference and the  $dV/dy$  magnitude diminished in the left as well as the right direction. On the contrary, for the with-wall-concavity case, the flow velocity increased in both the left and right directions, and a flow characterized by a large velocity gradient is induced for Type D60cu. Furthermore, the corresponding area is extended to  $x=40\text{mm}$  in comparison with that for Type D30n.

Next task is to study the mean absolute values of the jet-stream velocity-variation rate,  $|dV/dy|$ , for different channels with the diamond-shaped cylinder bundle. The corresponding results are depicted in Fig. 9 in the form of  $|dV/dy|$  versus  $Re_{\max}$  for five different types. Here,  $Re_{\max}$  is the maximum time-averaged velocity at the exit of channel, which is measured with the aid of Climomaster Anemometer (KANOMAX Co.). One observes that the magnitude of  $|dV/dy|$  is increased for each bundle and a substantial enhancement of  $|dV/dy|$  takes place at Type D60cu for the streamwise diverging diamond-shaped bundle. In contrast,  $|dV/dy|$  becomes lower for Type D30n and Type D30c, in which both results show slightly behavior with an increase in Reynolds number. Note that as the Reynolds number is increased, Type D60n, Type D60c and Type D60cu approach the similar value and produce a  $dV/dy$  approximately twice higher than in the absence of the wall concavity.

It is found from the present study that the diffusion phenomenon in the jet-stream is quantitatively disclosed by different bundle shapes. When the flip-flop flows is applied to the industrial area, PIV measurement discloses that the provision of the wall concavity produces a large flow change in the effluent flow field from diamond-shaped cylinder bundles and an enhancement in both the turbulence and dispersion of individual jet streams. This trend becomes larger by the shape and size of the concavities and the Reynolds number. In summary, the visualization studies of water and air jet streams have disclosed that the presence of the wall concavity has resulted in a large change in the flow in the efflux jet-stream field from the diamond-shaped cylinder bundle and large turbulence and dispersion of individual jet streams.

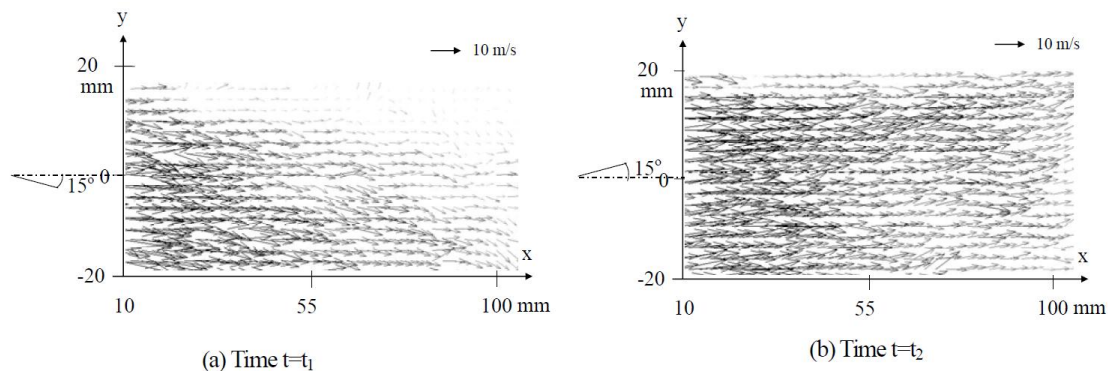


Fig. 7.1 Vector distributions of jet streams at an instant time for Type D30n ( $Re_{\max}=7,900$ )

FLOW VISUALIZATION OF FLIP-FLOP FLOWS  
INSIDE STREAMWISE DIVERGING DIAMOND-SHAPED CYLINDER BUNDLES

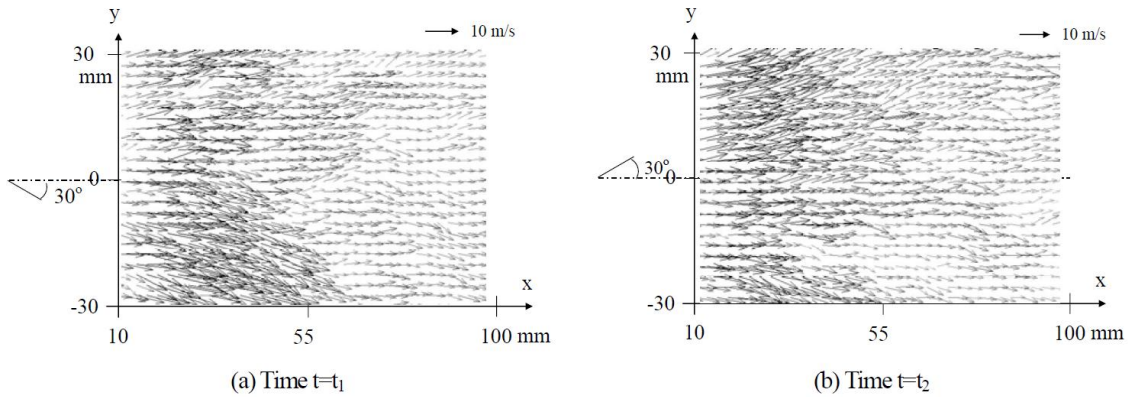


Fig. 7.2 Vector distributions of jet streams at an instant time for Type D60cu ( $Re_{max}=7,300$ )

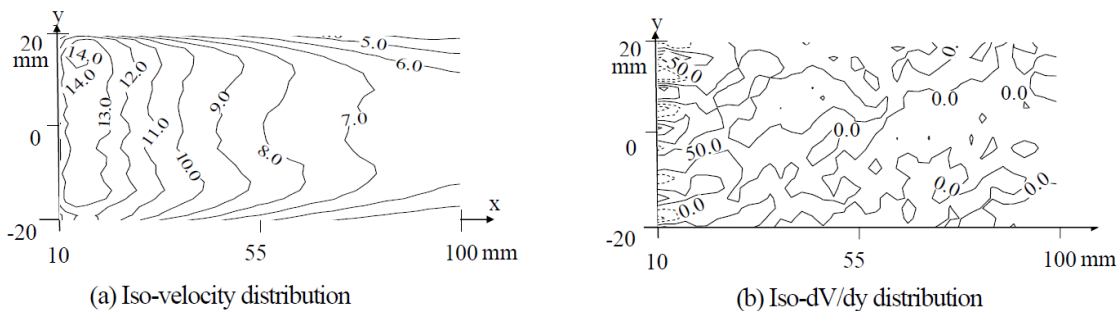


Fig. 8.1 Iso-velocity and iso-dV/dy distributions of jet streams for Type D30n ( $Re_{max}=7,900$ )

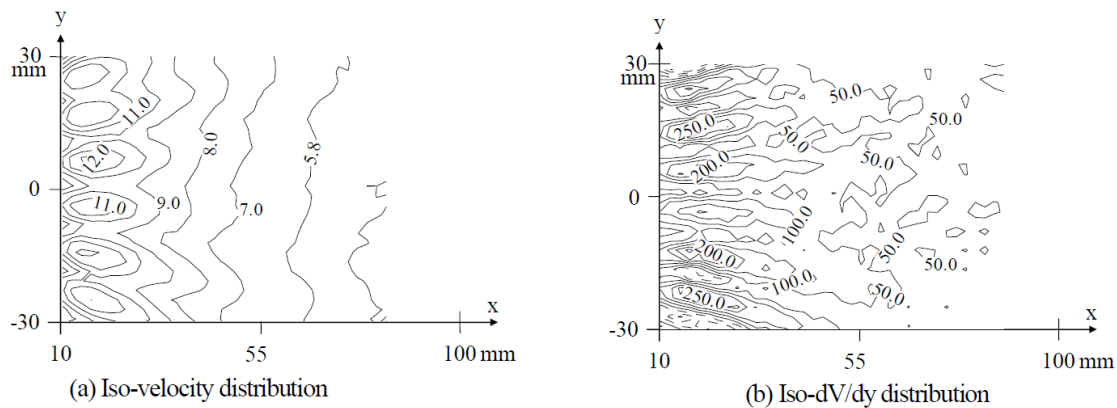


Fig. 8.2 Iso-velocity and iso-dV/dy distributions of jet streams for Type D60cu ( $Re_{max}=7,300$ )

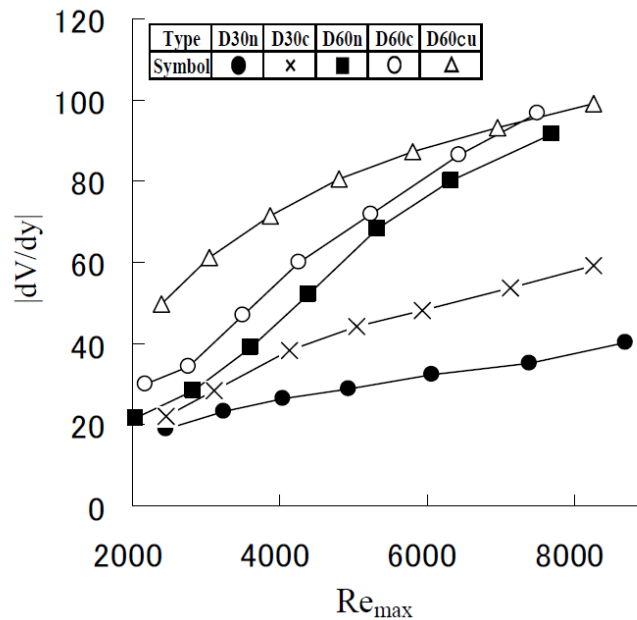


Fig. 9 Change of  $|dV/dy|$  versus  $Re_{max}$

#### 4 Summary

Using water and air as the test fluids, various visualization/measurement experiments have been performed to determine changes in flow inside and effluent from diamond-shaped cylinder bundles with and without wall concavity. Results have been summarized here:

- (1) Pressure loss characteristics are disclosed for Type D30 and Type D60 with and without wall concavity.
- (2) In the efflux jet streaklines, flip-flop flow oscillations occur with the appearance of large dispersion of the left- and right-ward air and water jet streams. Irrespective of with or without the wall concavity, flow in the horizontal efflux jet-stream field is almost symmetrical with respect to the central longitudinal line as the axis.
- (3) Suction effect is induced by the rotation of the vortex in the concavities constructed on both sidewalls inside the diamond-shaped cylinder bundle. Consequently, flip-flop flow oscillations is enhanced and its dispersion angle  $60^\circ$  for Type D60.
- (4) As for the mean absolute values of the jet-stream velocity-variation rate, the corresponding behavior is affected by Reynolds number and channel flow, i.e., Type D30 and Type D60.

In addition to the applications of these results to fluids-engineering equipment related to mixing, stirring, and washing such as pollutant dispersion, more efficient machinery can be developed.

#### Acknowledgment

The work was partially supported by Grant-in-Aid for Scientific Research (No. 22560180) from the Japan Society for Promotion of Science for which the authors wish to express their sincere gratitude.

## References

1. Zaman, K. B. M. Q., Reeder, M. F., and Samimy, M., Control of an axisymmetric jet using vortex generators, *Phys. Fluids*, vol. 6, no. 2, pp. 778–796, 1994.
2. Yokota, K. (Nagoya Institute of Technology), Patent no. 2008-207119, 2008.
3. Umeda, S. and Yang, W.-J., *Diagnosis of Intersecting Flow – on Visualization of Flow Networks-*, Kyoritsu Publishing Co. Ltd., p. 2, 2007.
4. Umeda, S., Hasegawa, S. and Yang, W.-J., Occurrence of flip-flop flows in diamond-shaped cylinder bundles, *J. Environ. Eng.*, vol. 2, no.1, pp. 1–12, 2007.
5. Umeda, S., Iijima, K., Shinmura, K. and Yang, W.-J., Effect of Wall Concavity on Oscilations of Jet Streams from Diamond-Shaped Cylinder Bundle, *J. Flow Visualization and Image Process.*, vol. 18, pp. 165-183, 2011.
6. Yang, W.-J. and Umeda, S., Coanda effect and its role in mixing in intersecting flow, *Proc. of CSME FORUM SCGM 1998*, vol. 1, pp. 147–152, 1998.
7. Umeda, S., Patent no. 2841173, 1998.
8. Umeda, S., Characteristics of intersecting flows in multiple diamond-shaped islands, *J. Flow Visualization and Image Process.*, vol. 8, pp. 165–176, 2001.